Tulchinsky and Peters outline the development of leukocyte receptor-binding radiotracers and describe requirements for ideal infection and inflammation imaging agents. . . . . ***Page 718***

Sciagrà and colleagues report on the use of gated SPECT to assess the effect of abciximab therapy on outcomes after myocardial reperfusion in patients with acute myocardial infarction. . . . ***Page 722***

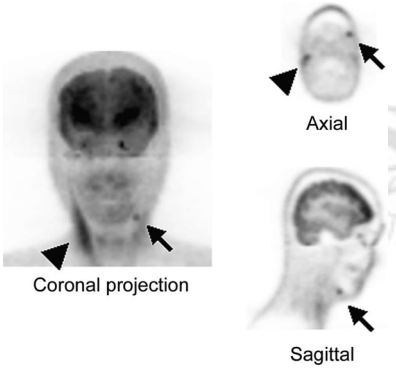

Slomka and colleagues apply delayed-enhancement MRI as a validation tool to measure the accuracy of a novel automated myocardial perfusion ^{201}Tl SPECT quantification method, based on normal limits, for detection and sizing of infarcts. . . . . ***Page 728***

Fricke and colleagues evaluate the enhanced accuracy of a SPECT/low-dose CT device in myocardial perfusion scintigraphy and compare results with those from ^{13}N-ammonia PET. . . . . ***Page 736***

van Dyck and colleagues use ^{123}I-β-CIT to investigate the relationship between striatal dopamine transporter (DAT) protein availability and a polymorphism of the gene that codes for DAT and discuss the implications of their findings for neuropsychiatric studies. . . . . ***Page 745***

Ishimori and colleagues report on the detection of unexpected ^{18}F-FDG–avid additional primary malignant tumors, as well as false-positive results, in patients being evaluated by whole-body ^{18}F-FDG PET/CT for known or suspected malignancies. . . . . ***Page 752***

Israel and colleagues study the nature and significance of unexpected focal ^{18}F-FDG uptake localized by PET/CT within the gastrointestinal tract in a retrospective review of more than 4,000 patients. . . . . ***Page 758***

Henze and colleagues describe the pharmacokinetic modeling of the high uptake of ^{68}Ga-DOTA-TOC in meningiomas and offer data that may serve as a basis for the use of PET in radiotherapy planning and subsequent monitoring of somatostatin receptors. . . . . ***Page 763***

Yen and colleagues evaluate the sensitivity and prognostic significance of whole-body ^{18}F-FDG PET for follow-up evaluation of recurrences and metastases in patients with nasopharyngeal carcinoma. . . . . ***Page 770***

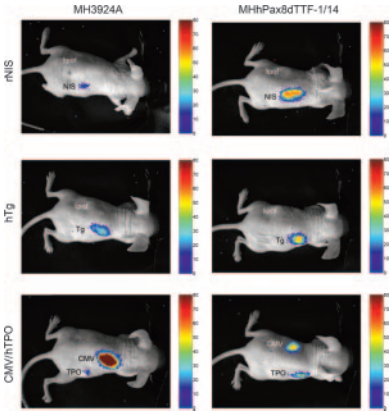

Yen and colleagues detail a study evaluating the utility of PET in staging untreated squamous cell carcinoma of the buccal mucosa and compare the results with those from CT and MRI and histopathology. . . . . ***Page 775***

Zitzmann and colleagues report on a novel bacterial peptide display system as an alternative to phage peptide display for the isolation of new prostate tumor–specific peptides. . . . . ***Page 782***

van Eerd and colleagues study the pharmacodynamics of ^{111}In-DPC11870 to determine the mechanism of accumulation of the radiolabeled LTB4 antagonist in infectious and inflammatory foci in an animal model. . . . . ***Page 786***

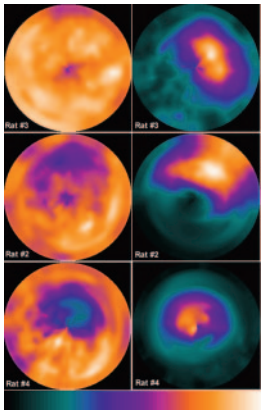

Takei and colleagues elucidate the relationship between apoptosis and glucose utilization during cancer chemotherapy using ^{99m}Tc-annexin V and ^{18}F-FDG and compare the uptake of these tracers in a rat tumor model. . . . . ***Page 794***

Semnani and colleagues assess the efficacy of targeting of lung metastases in mice with various formulations of the radioiodinated thymidine analog ^{123}I-IUdR/^{125}I-IUdR. . . . . ***Page 800***

Tait and colleagues look at ways in which changes in membrane-binding affinity, molecular charge, and method of labeling affect the biodistribution of ^{99m}Tc-annexin V in normal and apoptotic tissues. . . . . ***Page 807***

Zhou and colleagues describe the potential of dual-tracer small-animal SPECT in simultaneous imaging of ^{99m}Tc-sestamibi to

assess myocardial perfusion and of ^{111}In-labeled stem cells to delineate stem cell grafts in regions of infarct. . . . . ***Page 816***

Maina and colleagues compare the biologic profiles of ^{99m}Tc-demobesin 1 and ^{111}In-Z-070 using various gastrin-releasing peptide receptor (GRP-R)–expressing tissues of human and animal origin and discuss the implications for the development of bombesin analogs for GRP-R–targeting applications. . . . . ***Page 823***

Altmann and colleagues visualize functional protein-to-protein interaction as thyroid transcription factors induce reporter gene expression in rat hepatoma cells and report on the ability of these factors to induce endogenous thyroid-specific gene expression and iodide accumulation in nonthyroid tumor cells. . . . . ***Page 831***

Dewaraja and colleagues describe the accuracy of ^{131}I activity quantification and absorbed dose estimation when patient-specific, 3-dimensional methods are used for SPECT reconstruction and absorbed dose calculation and discuss the implications for advances in radioimmunotherapy. . . . . ***Page 840***

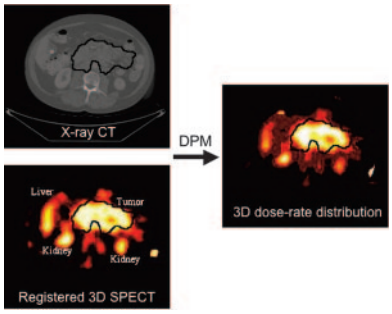

Vallabhajosula and colleagues evaluate the potential value of several factors in predicting myelotoxicity associated with ^{90}Y- and ^{131}I-labeled monoclonal antibody therapy in patients with prostate cancer. . . . . ***Page 850***

Brasse and colleagues use 3-dimensional whole-body PET simulations and phantom studies to investigate how gains in noise equivalent count rates from a noiseless random coincidence estimation method are translated to improvements in signal-to-noise ratio, with accompanying potential for reduction in scan duration. . . . . ***Page 859***

Seo and colleagues evaluate an iterative reconstruction algorithm using SPECT/CT data from phantoms and ^{111}In-capromab pendetide studies to assess the utility of a commercial SPECT/CT system in imaging of postprostatectomy patients at risk for residual or recurrent disease. . . . . ***Page 868***

Cheng and colleagues describe the use of matrix-assisted laser desorption/ionization time-of-flight mass spectrometry as a potential tool for high-throughput screening and characterization of molecular imaging probes or drug design and development. . . . . ***Page 878***

Froidevaux and colleagues evaluate the receptor-binding potency and biodistribution of radiolabeled analogs of α-melanocyte–stimulating hormone in a mouse melanoma model. . . . . ***Page 887***

ON THE COVER

In patients with known cancer, work-ups often focus on the primary disease, and incidental coexistence of another primary malignant lesion can be missed. The prevalence of additional primary neoplasms is substantial. Whole-body PET with ^{18}F-FDG has been used successfully and with increasing frequency in the evaluation and clinical management of an expanding number of neoplasms. Reports also indicate that ^{18}F-FDG PET has the potential for cancer screening and can detect new malignant tumors in a small fraction of asymptomatic individuals. Because PET/CT allows precise determination of the location of ^{18}F-FDG uptake, whole-body studies may be of value in the detection of unexpected additional primary malignant tumors in patients with known or suspected malignancies.